

**1 Impact of cloud microphysics on hurricane track**  
**2 forecasts**

Robert G. Fovell

**3** Department of Atmospheric and Oceanic Sciences, University of California,  
**4** Los Angeles, Los Angeles, CA, 90095-1565, USA.

Hui Su

**5** Jet Propulsion Laboratory, California Institute of Technology, Pasadena,  
**6** CA, 91109, USA.

---

Robert G. Fovell, Department of Atmospheric and Oceanic Sciences, University of California,  
Los Angeles, Los Angeles, CA, 90095-1565, USA. (rfovell@ucla.edu)

Hui Su, Jet Propulsion Laboratory, California Institute of Technology, Pasadena, CA, 91109,  
USA. (Hui.Su@jpl.nasa.edu)

7 Simulations of Hurricane Rita (2005) at operational resolutions (30 and  
8 12 km) reveal significant track sensitivity to cloud microphysical details, ri-  
9 valing variation seen in the National Hurricane Center's multi-model conen-  
10 sus forecast. Microphysics appears to directly or indirectly modulate vortex  
11 size and winds at large radius and possibly other factors involved in hurri-  
12 cane motion. Idealized simulations made at higher (3 km) resolution further  
13 demonstrate the microphysical influence.

## 1. Introduction

14 Official National Hurricane Center (NHC) statistics show that Atlantic Basin storm po-  
15 sition forecasts have improved markedly in recent decades. Yet, the 2005 season reminds  
16 us that much progress remains to be made. On the morning of September 24, 2005, Hur-  
17 ricane Rita made landfall near the Texas/Louisiana border as a Saffir-Simpson Category  
18 3 storm, with  $\sim 54 \text{ m s}^{-1}$  maximum winds. This location was correctly identified in the  
19 NHC forecast issued 36 hours prior to landfall but their 54 hour forecast had the highest  
20 probability landfall located west of Houston, a shift of more than 130 km. This prompted  
21 a frantic and, as it transpired, unnecessary evacuation of that area. This position dis-  
22 crepancy was about average when compared to recent years, but looms very large indeed  
23 when weighted by population.

24 Weather forecasts in general have made great use of ensemble forecasting, in which dif-  
25 ferent models, model physics options and/or initializations are applied to the same event,  
26 yielding an objective measure of forecast uncertainty. Previous work involving both real-  
27 data and idealized modeling has shown that the choice of cumulus parameterizations,  
28 boundary layer and/or cloud microphysics schemes can dramatically influence hurricane  
29 simulations, especially with respect to intensity and intensification rate, rainfall produc-  
30 tion and inner core structure (e.g., Willoughby et al. 1984; Lord et al. 1984; Karyampudi  
31 et al. 1998; Braun and Tao 2000; Wang 2002; McFarquhar et al. 2006; Zhu and Zhang  
32 2006). Regarding microphysics, Lord et al. (1984) found including ice processes resulted in  
33 a significantly stronger storm, while Wang (2002) and Zhu and Zhang (2006) showed that  
34 disallowing melting and evaporation permitted substantially more rapid intensification

35 and lower central pressures. However, sensitivity of hurricane track or propagation speed  
36 to cloud microphysics has either not been found in these studies or has gone unreported.

37 Herein, we demonstrate that microphysical assumptions can dramatically impact fore-  
38 casted track in Weather Research and Forecasting (WRF; Skamarock et al. 2007) model  
39 simulations of Hurricane Rita at “operational” resolutions of 30 km and 12 km. A more  
40 idealized model at finer resolution is used to examine the generality of the results.

## 2. The Operational Ensembles (30 and 12 km Resolution)

41 Most of the simulations employed WRF version 2.1.2 and a spatially extensive domain  
42 centered on the northern Caribbean. Four microphysical parameterizations (MP) were  
43 explored: the Kessler (“warm rain”), the Lin et al. (LFO), and the three and five class  
44 WRF single moment (WSM3 and WSM5) options. All but the Kessler scheme explicitly  
45 treat frozen water in some fashion. The Kain-Fritsch (KF), Grell-Devenyi and (from WRF  
46 2.0.3.1) Betts-Miller-Janjic (BMJ) convective parameterizations (CPs) were tested. Runs  
47 were also made with MP and/or CP schemes deactivated. The influence of subgrid-scale  
48 mixing was also explored, and found to affect intensity more than track in this experiment.

49 The operational simulations employed 31 vertical levels with a model top at 50 mb. Us-  
50 age of additional levels or a higher model tops were not found to materially affect hurricane  
51 motion. Initial and boundary data were provided by National Centers for Environmental  
52 Prediction Global Forecast System forecasts at one degree resolution, commencing either  
53 06 UTC or 18 UTC Sept. 22nd. In the 30 km ensemble, an LFO/KF simulation started  
54 at 18 UTC, about 39 hours prior to landfall, yielded accurate predictions (not shown) of

55 landfall location, storm width, timing and intensity (936 mb), in good agreement with  
56 the contemporaneous NHC forecast.

### 2.1. 30 km Ensemble Results

57 The physics-based ensemble experiment was conducted for the earlier initialization time.  
58 Figure 1 presents a sea-level pressure (SLP) track plot for the LFO/KF (control) run.  
59 At each point depicted, the lowest SLP recorded during the final 27 hours of the 54  
60 hour simulation, based on hourly data, is plotted. Similar to the contemporaneous NHC  
61 forecast, the control run's hurricane reached land near Houston. It reached a minimum  
62 SLP of less than 924 mb before weakening prior to reaching land; this minimum pressure is  
63 lower than actually measured at or subsequent to this time (931 mb). The track followed  
64 by the hurricane's eye is traced by the open circles, representing three-hourly positions  
65 ending at 12 UTC Sept. 24th, about three hours after the actual storm reached the coast.

66 Superposed are the best and worst results from this ensemble, as determined by position  
67 error. The WSM3/BMJ combination (filled squares) correctly simulated both landfall  
68 location and timing. In contrast, Kessler/KF member (filled circles) produced a weaker  
69 (minimum SLP 944 mb), more westward moving storm. Tracks from remaining members  
70 (not shown) generally fell between these two extremes. Taken together, this physics-based  
71 ensemble possessed a similar spread with respect to landfall as the NHC's multi-model  
72 ensemble did at this same time (also indicated on the figure). The NHC ensemble consists  
73 of over a dozen models of various types and levels of complexity.

## 2.2. 30 km Ensemble Sensitivity Tests

74 Microphysical parameterizations attempt to treat hydrometeors in bulk, based on pre-  
75 sumed particle size distributions, types and densities. Even the simplest schemes contain  
76 numerous assumptions and “knobs” that might lack observational or theoretical justifica-  
77 tion, and thus can be a source of uncertainty. To be *useful* uncertainty, each scheme has  
78 to have a reasonable chance of producing the most skillful result in any given situation,  
79 something a more extensive experiment might reveal. Since model physics can interact in  
80 complex and potentially unpredictable ways, the performance of various MP schemes and  
81 the impact of their inherent assumptions are likely case- and even resolution-dependent.

82 We have attempted to identify MP scheme “knobs” that excite the sensitivity seen  
83 above. The most significant difference between the Kessler scheme and any MP that  
84 considers ice is that the average particle fallspeed is likely smaller when frozen condensate  
85 is included. Fallspeed assumptions directly and indirectly influence particle growth rates,  
86 the horizontal spread of condensate and vertical heating profiles, potentially interacting  
87 strongly with how and where CP-based adjustments are triggered. To explore the role  
88 of hydrometeor fallspeed on the ensemble spread, we took the most accurate member  
89 (WSM3/BMJ) and forced ice to share the terminal velocity of raindrops having equivalent  
90 mass. This resulted in a simulated hurricane landfall to the *west* of Houston, shown on  
91 Fig. 1 as the short-dashed line, a considerable increase in position error.

92 The long-dashed line on the figure shows what transpired when the rainwater terminal  
93 velocity was set to zero in the Kessler scheme, effectively removing precipitation. This  
94 run’s position error was no worse than that of the control run. Without precipitation,

95 there is little to no evaporation cooling in the boundary layer. However, another modified  
96 Kessler run lacking only evaporation of rainwater possessed the same track as the origi-  
97 nal Kessler/KF storm. These results suggest that, at least for this particular situation,  
98 considerable sensitivity can be excited via manipulating hydrometeor fallspeeds.

### 2.3. 12 km Ensemble Results and Sensitivity Tests

99 To ascertain whether the microphysical influences found in the 30 km runs persist  
100 when the grid spacing is altered, we also conducted a full physics-based ensemble using  
101 12 km horizontal grid spacing. At this resolution, the WRF model is able to produce  
102 model hurricanes with realistic intensity without CP schemes, so those members will be  
103 highlighted below. Figure 2 shows SLP track plots for the 12 km Kessler, LFO and  
104 WSM3 runs. As in the 30 km ensemble, the Kessler scheme produced the weakest and  
105 most westward propagating hurricane, still making landfall well west of Houston. This  
106 was also clearly the widest vortex of the three. The WSM3 simulation again yielded the  
107 most accurate landfall while LFO microphysics maintained the deepest storm (929 mb).  
108 All of the 12 km runs made without CP schemes tended to make landfall a few hours late.

109 While the basic MP dependencies are similar at this higher operational resolution, some  
110 of the specific sensitivities differ from their 30 km counterparts. For example, at 12 km  
111 and without active CP, altering the rainwater terminal velocity in the Kessler scheme  
112 had far less impact on the landfall location (not shown). At 30 km, that alteration was  
113 perhaps exaggerated owing to interaction with the cumulus parameterization, which was  
114 more critical to vortex development and maintenance at that coarser grid spacing. The  
115 substantial influence regarding ice fallspeed previously encountered (in the WSM3/BMJ

116 experiment) was also largely absent at higher resolution in the absence of a CP. Yet, other  
117 sensitivities were discovered. Fig. 2d shows what transpired when the WSM3 scheme was  
118 modified to neglect the latent heat of fusion, the extra  $\sim 10\%$  heating that occurs when  
119 vapor converts directly to ice. The resulting hurricane was wider, weaker and made  
120 landfall at Houston. The same alteration in the 30 km experiment had little effect on  
121 track, at least when a CP scheme was active.

## 2.4. Synthesis

122 Considering the 30 and 12 km results jointly, we see that that microphysical assumptions  
123 can exert a significant influence on hurricane track over relatively short ( $\sim 54$  h) time  
124 scales. Microphysics may influence storm motion by directly or indirectly encouraging  
125 different vortex asymmetries. One such asymmetry results from the latitudinal gradient  
126 of planetary vorticity, the “beta effect” and its secondary circulation (e.g., Holland 1983;  
127 Chan and Williams 1987; Fiorino and Elsberry 1989) that makes relatively larger vortices  
128 more likely to drift northwestward (Holland 1984; DeMaria 1985). Figure 3 shows vortex-  
129 following composites of 850 mb absolute vorticity for the 12 km ensemble’s Kessler and  
130 WSM3 members, demonstrating again the size difference between the two storms.

131 Persistent convective asymmetries can also influence vortex motion by inducing flow  
132 across the vortex towards the enhanced diabatic heating (Willoughby 1992; Wang and  
133 Holland 1996). Superposed on Fig. 3 is the asymmetric component of tropospheric aver-  
134 age ascent, a good proxy for convective heating. The negative values (dashed contours)  
135 in this field represent relatively weaker rising motion. For both storms, a dipole pattern  
136 is revealed, but the WSM field is rotated clockwise relative to the Kessler pattern, pos-

137 sibly assisting the former's relatively more poleward motion. In any event, among these  
138 simulations anything that is done to narrow the vortex, whether it becomes more intense  
139 as a result or not, tends to permit the hurricane to propagate more northward. In the  
140 case of Rita, at least, that resulted in a more accurate landfall.

### 3. The "Waterworld" Experiments

141 Hurricanes often move through complex and dynamic environments, complicating anal-  
142 ysis of the microphysical impacts on simulated track and intensity. To isolate these in-  
143 fluences, a modified real-data version of WRF version 2.2 called "Waterworld" (WW)  
144 was created which retains Earth's rotation and (optionally) curvature, but has no land, a  
145 uniform SST of 29°C and a calm, horizontally homogeneous base state based on Jordan's  
146 (1958) hurricane season composite. Waterworld employs three telescoping domains, the  
147 outer spanning 3240 km by 3240 km with 27 km resolution and the innermost being 669  
148 km on a side with 3 km grid spacing. The outer domain is intended to capture the en-  
149 tire environmental response to the hurricane; its boundary conditions are fixed, and thus  
150 effectively closed.

151 The operational real-data simulations commenced with a pre-existing vortex and no  
152 condensation. Idealized simulations often start off with an artificially imposed circulation  
153 (e.g., Wang 2002; Kimball and Evans 2002) . We elected to "breed" a vortex by placing  
154 a warm, moist bubble centered at 20°N and integrating for a spin-up period of 24 hours  
155 with the Kain-Fritsch CP scheme active in all domains and microphysics switched off.  
156 During this period, a coherent and well-resolved cyclone formed, achieving a central SLP  
157 of 969 mb by 24 hours. At that time, experiments continued with either the CP scheme

158 or one of three MP schemes (Kessler, LFO or WSM3) active. Each storm dealt only with  
159 environmental heterogeneity that it itself created.

160 Figure 4 shows results from an experiment retaining Earth curvature (having variable  
161 Coriolis parameter  $f$ ). Despite sharing a common initial condition, the storms quickly  
162 diverged with respect to track, propagation speed and intensity. As in the real-data runs,  
163 the Kessler vortex tracked farthest to the west, the WSM3 storm moved most northward,  
164 and the LFO simulation fell in between. A very substantial propagation speed difference  
165 is also evident. At 54 h after the end of the spin-up period, the Kessler vortex' forward  
166 motion was  $9 \text{ km h}^{-1}$  and increasing. At that time, the LFO and WSM3 storms were  
167 moving 43% and 52% slower, respectively. Recall there was no initial environmental flow,  
168 so this is entirely self-propagation. When combined with track variations, position differ-  
169 ences among the simulated storms soon became extremely large. The rapid movement of  
170 the Kessler vortex relative to the ice MP storms is the most substantial difference with  
171 respect to the real-data Rita runs. Quantitatively similar direction and speed disparities  
172 were noted in a lower (12 km) resolution version of WW (not shown).

173 With regard to intensity, the Kessler (LFO) vortex was weakest (strongest) of the MP  
174 runs, again consistent with the real-data runs. The inset on Fig. 4 shows radial profiles  
175 of the 10 m wind speed taken at the 54 hour mark. The LFO storm was still intensifying  
176 at this time, and spent over 2 days at or very near Category 5 intensity, while the warm  
177 rain vortex fluctuated between Categories 2 and 3. The warm rain storm had the most  
178 radially expansive circulation, and was thus again the most influenced by beta drift. The  
179 translation speed differences may reflect the variation in wind speeds seen at large radius,

180 as suggested by Fiorino and Elsberry (1989). As expected, none of the model storms  
181 translated significant distances in an  $f$ -plane version of this experiment located at 20°N  
182 (not shown). The Kessler vortex was weaker, had a wider eye, and stronger winds at large  
183 radius than the LFO storm but this had no effect on translation.

#### 4. Summary and Conclusions

184 Hurricane track and landfall forecasting is a complex scientific problem with significant  
185 societal import. Herein, it was demonstrated variation of cloud microphysical processes,  
186 performed in the context of ensemble forecasting at operational resolutions, can yield an  
187 ensemble spread comparable to multi-model ensembles, possibly by directly and indirectly  
188 modulating vortex size and structure. Indeed, it is possible that the differences among  
189 various dynamical models could chiefly reside in their respective handling of microphysics,  
190 along with other processes related to convection. The uncovered sensitivities were found to  
191 vary somewhat with resolution, possibly owing to a subtle interplay among model physics,  
192 and are deserving of a more comprehensive examination. Still, microphysics appears to  
193 be one avenue to exciting the inherent propagation sensitivity of hurricane-like vortices  
194 and should be considered as a valuable part of physics-based ensemble forecasting.

195 **Acknowledgments.** This work was supported by NSF grant ATM-0554765. We ac-  
196 knowledge the support by the Jet Propulsion Laboratory, California Institute of Technol-  
197 ogy, sponsored by NASA, and The Aerospace Corporation. The single-sounding WRF ini-  
198 tialization used in “Waterworld” was designed by Gary Lackmann and Kevin Hill (North  
199 Carolina State Univ.). Jonathan Vigh (Colorado State Univ.) provided the NHC ensem-  
200 ble track data.

## References

- 201 Braun S. A., W.-K. Tao, 2000: Sensitivity of high-resolution simulations of Hurricane Bob  
202 (1991) to planetary boundary layer parameterizations. *Mon. Wea. Rev.*, **128**, 39413961.
- 203 Chan, J. C.-L., and R. T. Williams, 1987: Analytical and numerical studies of the beta-  
204 effect in tropical cyclone motion. *J. Atmos. Sci.*, **44**, 1257-1265.
- 205 DeMaria, M., 1985: Tropical cyclone motion in a nondivergent barotropic model. *Mon.*  
206 *Wea. Rev.*, **113**, 1999-2110.
- 207 Fiorino M. J., and R. L. Elsberry, 1989: Some aspects of vortex structure related to  
208 tropical cyclone motion. *J. Atmos. Sci.*, **46**, 975-990.
- 209 Holland, G. J., 1983: Tropical cyclone motion: Environmental interaction plus a beta  
210 effect. *J. Atmos. Sci.*, **40**, 328-342.
- 211 Holland, G. J., 1984: Tropical cyclone motion: A comparison of theory and observation.  
212 *J. Atmos. Sci.*, **41**, 68-75.
- 213 Jordan C. L., 1958: Mean soundings for the West Indies area. *J. Meteor.*, **15**, 9197.
- 214 Karyampudi, V. M., G. S. Lai, J. Manobianco, 1998: Impact of initial conditions, rain-  
215 fall assimilation, and cumulus parameterization on simulations of Hurricane Florence  
216 (1988). *Mon. Wea. Rev.*, **126**, 30773101.
- 217 Kimball S. K., and J. L. Evans, 2002: Idealized numerical simulations of hurricanetrough  
218 interaction. *Mon. Wea. Rev.*, **130**, 22102227.
- 219 Lord S. J., H. E. Willoughby, and J. M. Piotrowicz, 1984: Role of a parameterized ice-  
220 phase microphysics in an axisymmetric, nonhydrostatic tropical cyclone model. *J. At-*  
221 *mos. Sci.*, **41**, 2836-2848.

- 222 McFarquhar G. M., H. Zhang, G. Heymsfield, R. Hood, J. Dudhia, J. B. Halverson, F.  
223 Marks, 2006: Factors affecting the evolution of Hurricane Erin (2001) and the distribu-  
224 tions of hydrometeors: role of microphysical processes. *J. Atmos. Sci.*, **63**, 127-150.
- 225 Skamarock, W. C. and co-authors, 2007: A description of the Advanced Research WRF  
226 Version 2. *NCAR Tech. Note*, NCAR/TN-468+STR, 88pp.
- 227 Wang B., and G. J. Holland, 1996: The beta drift of baroclinic vortices. Part II: Diabatic  
228 vortices. *J. Atmos. Sci.*, **53**, 37373756.
- 229 Wang Y., 2002: An explicit simulation of tropical cyclones with a triply nested movable  
230 mesh primitive equation model: TCM3. Part II: Model refinements and sensitivity to  
231 cloud microphysics parameterization. *Mon. Wea. Rev.*, **130**, 30223036.
- 232 Willoughby, H. E., 1992: Linear motion of a shallow-water barotropic vortex as an initial-  
233 value problem. *J. Atmos. Sci.*, **49**, 2015-2031.
- 234 Willoughby H. E., H. Jin, S. J. Lord, and J. M. Piotrowitz: 1984: Hurricane structure and  
235 evolution as simulated by an axisymmetric, nonhydrostatic numerical model. *J. Atmos.*  
236 *Sci.*, **41**, 1169-1186.
- 237 Zhu, T., and D.-L., Zhang, 2006: Numerical simulation of hurricane Bonnie (1998). Part  
238 II: Sensitivity to varying cloud microphysical processes. *J. Atmos. Sci.*, **63**, 109-126.

239 **Figure Captions**

240 **Figure 1.** SLP track plot for the 30 km control (LFO/KF) run commencing 06 UTC  
241 Sept. 22nd, covering the final 27 hours of the 54 hour simulation; contour interval 8 mb.  
242 Tracks from selected ensemble members are superposed. Markers denote eye positions  
243 every three hours ending 12 UTC Sept. 24th. Only part of the domain is shown. Landfall  
244 area encompassed by NHC ensemble members reaching the coast by 12 UTC Sept. 24th  
245 is highlighted.

246 **Figure 2.** As in Fig.1, but for selected members of the 12 km ensemble. Only part of  
247 the domain is shown.

248 **Figure 3.** Vortex following composites for the 12 km Kessler and WSM3 members,  
249 constructed between forecast hours 48-54h, inclusive. Colored field is 850 mb absolute  
250 vorticity (units  $10^{-5} \text{ s}^{-1}$ ); contoured is the asymmetric component of tropospheric average  
251 ascent ( $0.1 \text{ m s}^{-1}$  contours, negative values dashed). Black dot marks eye location.

252 **Figure 4.** Three-hourly positions for 3 km Waterworld storms employing Kessler (K),  
253 LFO (L) and WSM3 (W) microphysics, commencing 12 hours after end of spin-up period.  
254 Positions and central pressures after 54 hours are highlighted. Inset shows radial profiles  
255 of 10 m wind speed vs. distance from eye for the three cases at 54 hours after spin-up.

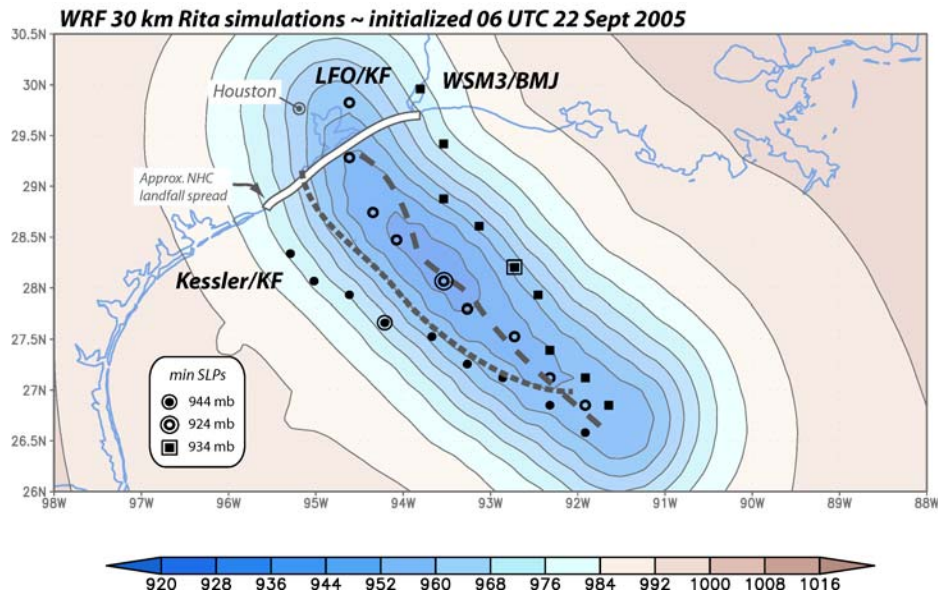


**Figure 1.** SLP track plot for the 30 km control (LFO/KF) run commencing 06 UTC Sept. 22nd, covering the final 27 hours of the 54 hour simulation; contour interval 8 mb. Tracks from selected ensemble members are superposed. Markers denote eye positions every three hours ending 12 UTC Sept. 24th. Only part of the domain is shown. Landfall area encompassed by NHC ensemble members reaching the coast by 12 UTC Sept. 24th is highlighted.

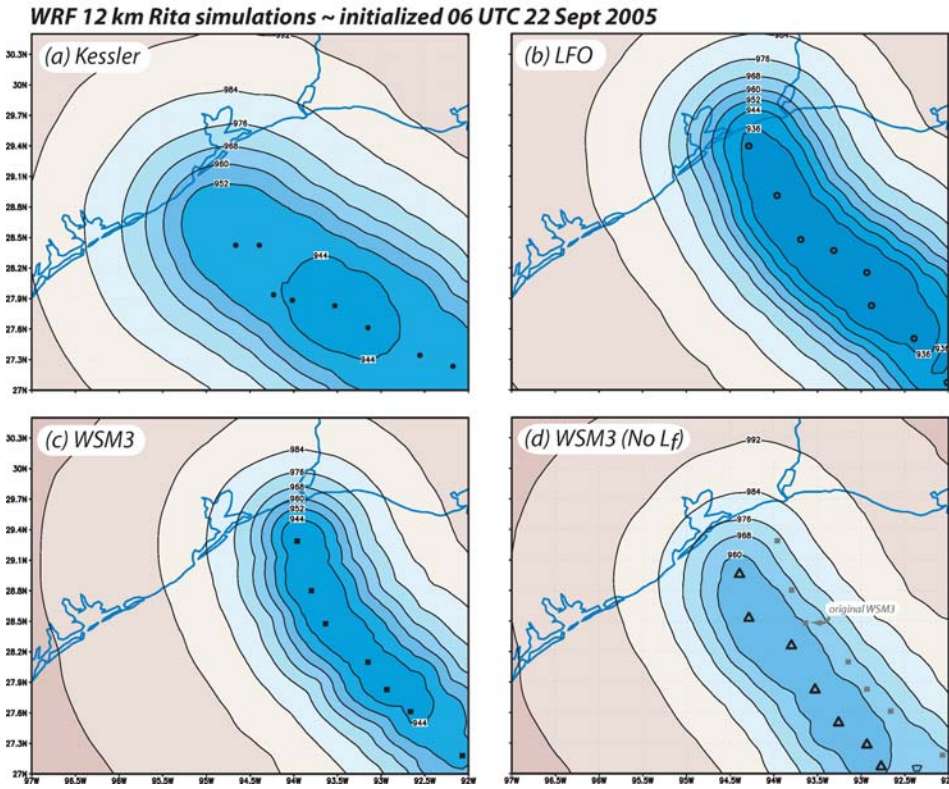


Figure 2. As in Fig. 1 but for selected members of the 12 km ensemble. Only part of the domain is shown.

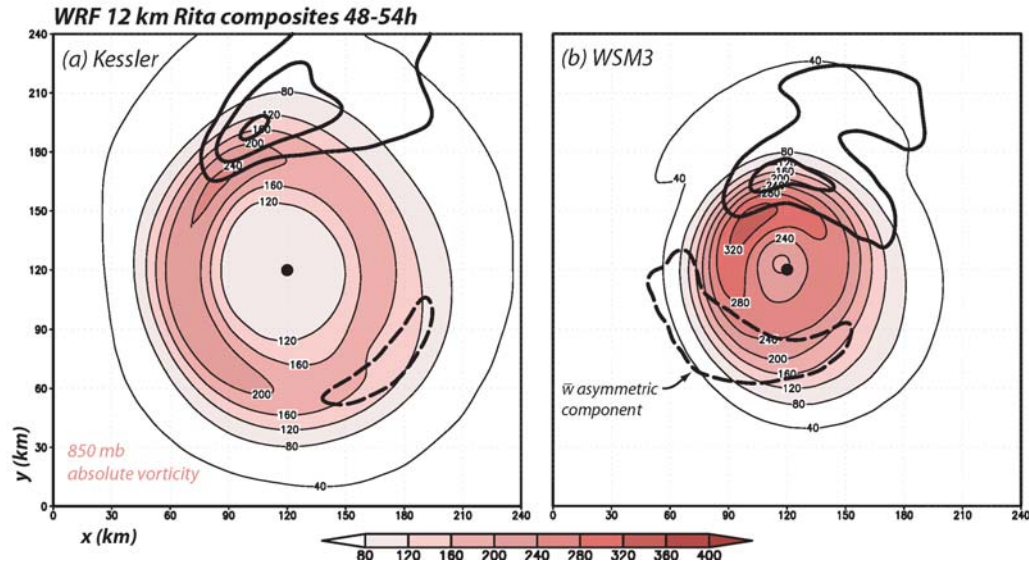
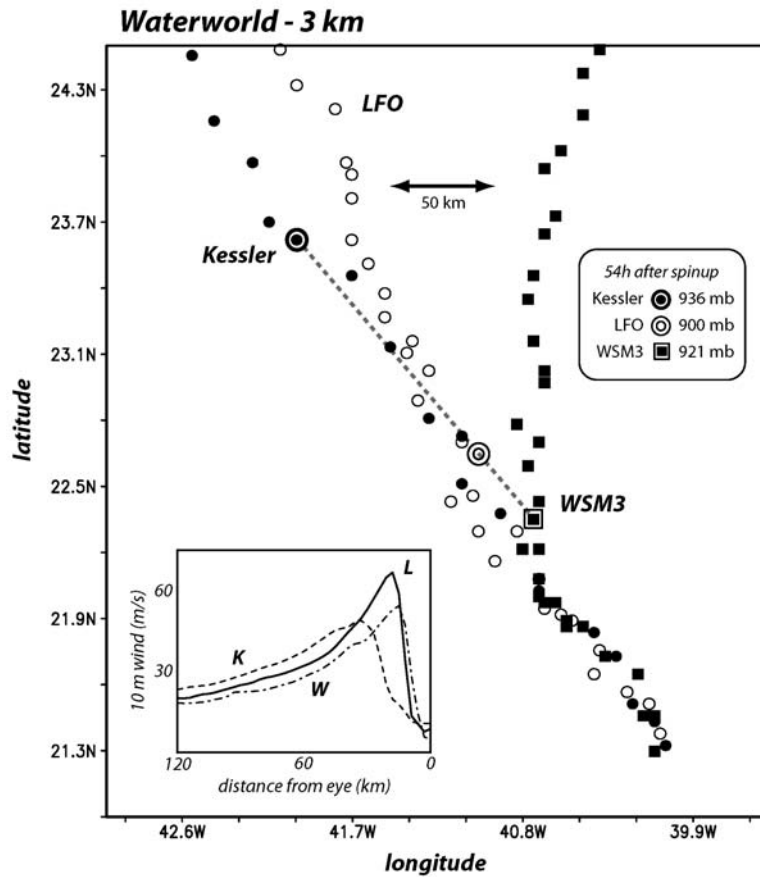


Figure 3. Vortex following composites for the 12 km Kessler and WSM3 members, constructed between forecast hours 48-54h, inclusive. Colored field is 850 mb absolute vorticity (units  $10^{-5} \text{ s}^{-1}$ ); contoured is the asymmetric component of tropospheric average ascent ( $0.1 \text{ m s}^{-1}$ , negative values dashed). Black dot marks eye location.



**Figure 4.** Three-hourly positions for 3 km Waterworld storms employing Kessler (K), LFO (L) and WSM3 (W) microphysics, commencing 12 hours after end of spin-up period. Positions and central pressures after 54 hours are highlighted. Inset shows radial profiles of 10 m wind speed vs. distance from eye for the three cases at 54 hours after spin-up.